

Influence of high-electronegativity atoms on the ^7Be decay rate

Farshid Gholamian  and Mohammad Mehdi Firoozabadi 

Department of Physics, Faculty of Sciences, University of Birjand, Birjand, Iran

Heidar Raissi

Department of Chemistry, Faculty of Sciences, University of Birjand, Birjand, Iran



(Received 23 October 2019; revised 17 May 2020; accepted 9 June 2020; published 9 July 2020)

First-principle calculations within the density-functional theory framework are used to study the effect of high electronegativity atoms on decay rate of the ^7Be nucleus. In this study, the electron-capture decay rate of the ^7Be nucleus is investigated in $\text{Be}(\text{OH})_2$, BeF_2 , BeF_3 , BeF_4 , BeCl_2 , BeCl_3 , BeCl_4 , C_{36} , and C_{60} species. It was found that the more decrease of the ^7Be decay rate was estimated in the BeF_4 (2.04%) and BeCl_4 (1.99%) relative to the Be metal. Furthermore, the half-life of ^7Be is different in various positions within C_{36} and C_{60} . The ^7Be half-life in $^7\text{Be}@\text{C}_{36}$ is greater than that in other fullerene compounds investigated, while the ^7Be half-life inside C_{60} is smaller.

DOI: [10.1103/PhysRevC.102.014606](https://doi.org/10.1103/PhysRevC.102.014606)

I. INTRODUCTION

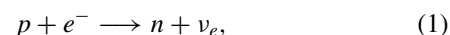
Although decay rate of an unstable nuclide is reported by a constant number in nuclear physics textbooks, it might be changed by putting the radioactive nucleus in different chemical environments. In the electron-capture (EC) process, a proton transforms into a neutron by capturing an electron from atomic layers. In 1947, Segrè [1] and Daudel [2] independently suggested that the decay rate of radioactive matter is proportional to electron density near the nucleus, which can be sensitive to the chemical composition.

In the case of light elements such as ^7Be that decays to ^7Li by the EC process, the decay rate appears to change by a considerable amount. For example, the decay rate of ^7Be is reported in the BeO compound to change by up to 1.5% [3–5]. Moreover, a theoretical study was performed on the electron density at the ^7Be nucleus in BeO and $\text{Be}(\text{OH})_2$ structures [6]. In the $\text{Be}^{2+}(\text{OH}_2)_4$, where ^7Be is surrounded by four water molecules in the solution, the decay rate changes by 0.7% [5,7,8]. Furthermore, half-life measurements were performed by inserting ^7Be into the following materials: Pd [9], In [9], Al_2O_3 [10], Au [10], Cu [11], and graphite [12].

After the discovery of C_{60} in 1985 [13], it was found that there are three ways to dope an atom into fullerenes: (a) doping inside the fullerene (endohedral fullerenes), (b) doping outside the fullerene (exohedral fullerenes), and (c) doping by substituting carbon atoms with other atoms (hetero fullerenes). Fullerenes smaller than C_{60} , such as C_{36} , are unstable and very reactive since they have adjacent pentagon pairs, and are not in good agreement with the isolated pentagon rule (IPR). These molecules are attractive for scientists

because of the existence of unique physical and chemical features such as their high electron affinity, which are predicted to be about 2.5 [14] and 2.68 eV [15], respectively. The C_{60} fullerene with bond lengths of 1.36 and 1.44 Å, has the I_h symmetry and is in the form of a hollow sphere. The C_{36} has D_{6h} in the highest allowed molecular symmetry, with bond lengths of 1.40 and 1.44 Å. From 2004, half-life of the ^7Be was measured in the C_{60} cage [16–18]. Also, theoretical studies of the ^7Be decay-rate changes in fullerenes are performed in Ref. [19–22].

The EC decay can be represented by the nuclear reaction



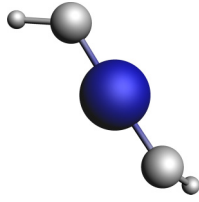
where p , e , n , ν_e are the proton, bound electron, neutron, and electron neutrino, respectively. Given the small size of nucleus, the nuclear wave functions are not affected by the chemical environment, so the variation of EC decay rate, $d\lambda_{EC}$, can be represented as [23]

$$d\lambda_{EC} = \left(\frac{\rho_e}{\rho_{e_{\text{ref}}}} - 1 \right) \lambda_{\text{ref}}, \quad (2)$$

where ρ_e is the electron density at the nucleus. According to Eq. (2), the change in the decay rate is approximately proportional to the electron-density difference at the nucleus. One may be expected to decrease of electron density at the Be nucleus by interactions with high electronegativity atoms, since $2s$ electrons of the Be atom are generally moved toward them.

In the present paper, quantum calculations are performed to obtain information from system properties such as the electron density at the nucleus. Interaction of the Be atom with high electronegativity atoms is investigated to obtain the relative decay-rate difference of the ^7Be at different compounds.

*mfiroozabadi@birjand.ac.ir

FIG. 1. The single-molecule structure of $\text{Be}(\text{OH})_2$.

II. CALCULATION PROCEDURE

Ab initio calculations are usually carried out by using density-functional theory (DFT) [19,24,25] or within the Hartree-Fock (HF) framework [20–22]. Both methods can be successfully described the electrical and structural properties of various chemical compounds. In the present study, *ab initio* computations are performed within DFT framework. The accuracy of DFT calculations depends on the approximation of the exchange-correlation (XC) functional; therefore, the meta generalized gradient approximation (meta-GGA) is used with the Minnesota 2006 local functional (M06-L). M06-L is one of the most accurate local functionals currently available and has good performance for both main groups and transition metals, inorganic and organometallics chemistry [26].

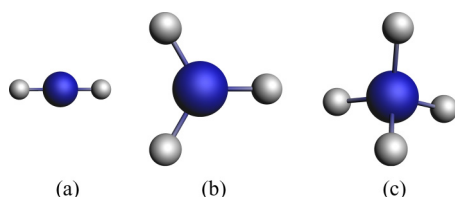
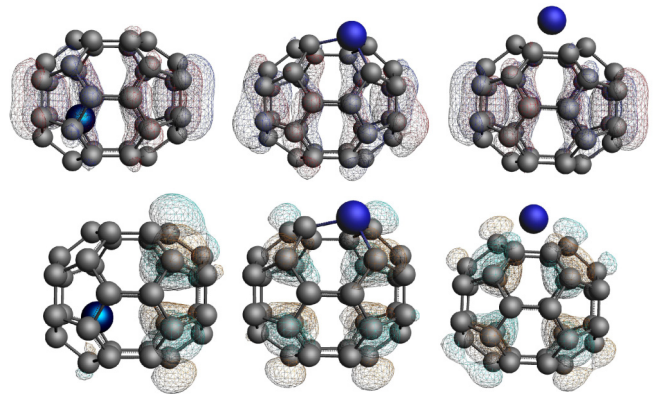
All the calculations have been performed by using the Amsterdam Density Functional (ADF) package [27]. The program uses Slater-type orbitals (STOs) that describe the electron wave functions at the nucleus (cusp like) better than Gaussian-type orbitals (GTOs). All-electron quadruple zeta plus four polarization (QZ4P) functions, which is the largest and most accurate basis set, are used to investigate the electronegativity effect of atoms on the decay rate of ^7Be . Electron density at the Be nucleus can be determined upon geometry optimization. Average electron density at the Be nucleus is calculated within a 2.98 fm radius around the center of the Be nucleus.

III. RESULTS AND DISCUSSION

A. Influence of the interaction of Be atom with high electronegativity atoms on the half-life of ^7Be nucleus

The oxygen (3.44), fluorine (3.98), and chlorine (3.16) atoms have more electronegativity than other elements. The Be atom loses a significant fraction from electrons by interacting with them. Electron density at the ^7Be nucleus in the BeO sample is changed by 1.5% relative to Be metal, which is in good agreement with experimental data in Ref. [5].

In the optimized single-molecule structure of $\text{Be}(\text{OH})_2$ (Fig. 1), each Be atom interacts by two hydroxide ions with

FIG. 2. The optimized structure of (a) BeF_2 , (b) BeF_3 , and (c) BeF_4 .FIG. 3. The equilibrium positions of ^7Be and isosurface plots of the HOMO (top) and the LUMO (bottom) in C_{36} .

electron affinity of 1.83 eV [28]. The result of calculations shows that decay rate of the ^7Be is decreased by about 1.3% and 1.66% in the single-molecule and the crystalline structure of $\text{Be}(\text{OH})_2$, respectively.

Furthermore, decay-rate change of the ^7Be nucleus is predicted by about -1.78% and -1.74% in the crystalline structure (-1.46% and -1.37% in the single molecule) of BeCl_2 and BeF_2 , respectively. Moreover, electron density at the ^7Be nucleus in calculated crystalline structures is smaller than in single-molecule structures, which is due to the existence of the high electronegativity atoms in crystalline structures.

Moreover, electron density at the ^7Be nucleus is calculated in BeF_2 , BeF_3 , and BeF_4 structures (Fig. 2). Results show that the difference of the ^7Be decay rate is estimated at -1.37% , -1.73% , and -2.04% , respectively. The more decrease in the electron density at the ^7Be nucleus is observed with the more increase in the number of F atoms.

B. Electron density at the Be atom in doped fullerenes

The electron affinity effect of fullerenes on the decay rate of ^7Be is estimated by finding the equilibrium position of the Be ion in the C_{36} and C_{60} (see Figs. 3 and 4, respectively). It was found that the Be position inside of the C_{60} is in the center of the fullerene, while for the C_{36} , it moves toward the center of one of the six pentagons. When a carbon atom is substituted with a beryllium atom, the average bond length between Be and C atoms (1.73 Å) is longer than C atoms (1.42 Å); therefore, one might expect that the symmetry of the C_{36} and C_{60} is lost.

Furthermore, isosurface plots of the highest occupied molecular orbital (HOMO) and the lowest unoccupied molecular orbital (LUMO) in C_{36} and C_{60} are shown in Figs. 3 and 4, respectively. It is found that the $\text{Be}@\text{C}_{60}$, $\text{Be}-\text{C}_{60}$, and $\text{Be}-\text{C}_{36}$ structures have an orbital localized around the Be ion, which shows that it is just an isolated ion in these structures. Also, the position of the HOMO moves with beryllium in the $\text{Be}@\text{C}_{36}$ structure, while the position of the LUMO shifts to the other side (Fig. 3, left). Because the Be atom has two fewer electrons than the C atom, two holes should be doped in the HOMO energy levels of BeC_{59} and BeC_{35} . In these

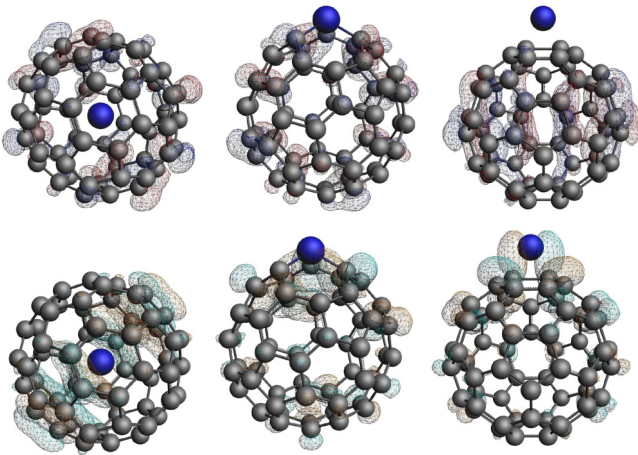


FIG. 4. The equilibrium positions of ${}^7\text{Be}$ and isosurface plots of the HOMO (top) and the LUMO (bottom) in C_{60} .

structures, isosurfaces of the HOMO are localized on C atoms, and isosurfaces of the LUMO are near the Be atom.

Results of the electron density for Be-doped fullerenes are summarized in Table I. The half-life of the ${}^7\text{Be}$ is drastically different in both fullerenes. When ${}^7\text{Be}$ is encapsulated in C_{60} , the electron density at the ${}^7\text{Be}$ nucleus is drastically increased relative to other positions in C_{60} , while it is decreased for C_{36} . Furthermore, our results confirm that the largest decay rate is obtained for ${}^7\text{Be}$ inside of the C_{60} molecule, which is in good agreement with the results reported in Ref. [20]. The increase of the ${}^7\text{Be}$ decay rate in ${}^7\text{Be}@C_{60}$ might be due to the existence of the 60 π electrons of C_{60} , as suggested in Ref. [16]. Also, the lowest decay rate of the ${}^7\text{Be}$ nucleus can be observed in the ${}^7\text{Be}@C_{36}$ compound; therefore, its half-life is the largest in comparison with other compounds, which is in good agreement with Ref. [21]. This can be due to the interaction of ${}^7\text{Be}$ with C atoms.

Moreover, results of the electron-density calculation are compared in Fig. 5. Decay rate of the ${}^7\text{Be}$ nucleus is more decreased in the ${}^7\text{Be}@C_{36}$, BeF_4 , and BeCl_4 . Also, our results indicate that the electron density in ${}^7\text{Be}-\text{C}_{36}$ and ${}^7\text{Be}-\text{C}_{60}$ is close to the electron density in the Be ion, which is due to the weaker interaction of the Be atom with fullerenes.

C. The Bader charge analysis

To understand that why the electron density at the ${}^7\text{Be}$ nucleus is varied by changing the geometrical position of the

TABLE I. Electron densities at the Be nucleus in doped fullerenes.

Structure	ρ_e (e/Bohr^3)
${}^7\text{Be}@C_{36}$	34.93
${}^7\text{BeC}_{35}$	35.15
${}^7\text{Be}-\text{C}_{36}$	35.13
${}^7\text{Be}@C_{60}$	35.93
${}^7\text{BeC}_{59}$	35.16
${}^7\text{Be}-\text{C}_{60}$	35.19

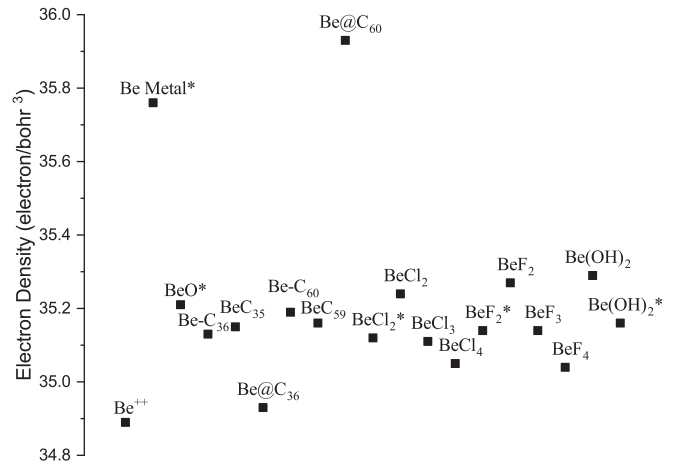


FIG. 5. Calculated electron density at the ${}^7\text{Be}$ nucleus in different compounds (* shows that this structure is in the crystalline form).

Be atom in the fullerene, it is attractive to perform the Bader charge analysis on the Be atom in these structures. Results of the calculated electron density at the ${}^7\text{Be}$ nucleus, variation of the decay rate of ${}^7\text{Be}$, and the Bader charge analysis are presented in Table II.

The Bader charge analysis gives an estimate of the charge distribution in the structures. In this analysis, molecules are divided into atom-like fragments based on the quantum theory of atoms in molecules (QTAIM), which provides a method in terms of electron density [29]. The maximum electron density occurs at the nucleus due to the source of the positive charge. The gradient of the electron density is positive in the space of atoms. The minimum electron density along the bond path is called the bond critical point which separated atoms in a molecule [30].

Results of the calculated electron density at the ${}^7\text{Be}$ nucleus, variation of the decay rate of ${}^7\text{Be}$, and the Bader charge analysis are presented in Table II. According to the results of the Bader charge analysis, the electron density at the ${}^7\text{Be}$ nucleus is generally increased by increasing the Be charge in the structure. However, there are some deviations from the expected relation in the approximately same results. The Bader charge estimates the electronic charge of atoms in molecules, while electron density is calculated at the nucleus.

TABLE II. Electron densities at the Be nucleus compared with the Bader charge analysis.

Structure	ρ_e (e/Bohr^3)	$d\lambda_{EC}$	Bader charge
Be metal ^a	35.76	Ref.	4
Be^{++}	34.89	-2.43	2
BeO^a	35.21	-1.54	2.26
$\text{Be}@C_{60}$	35.93	0.48	3.83
BeCl_2^a	35.12	-1.79	2.28
BeF_2^a	35.14	-1.73	2.23
BeF_4	35.03	-2.04	2.21
$\text{Be}(\text{OH})_2^a$	35.16	-1.68	2.24

^aStructure is in the crystalline form.

Therefore, correlation of these parameters can be removed in such results. For example, electron density at the ${}^7\text{Be}$ in BeCl_2 is less than BeF_2 . This deviation is probably due to difference of structure in BeCl_2 and BeF_2 . BeCl_2 has a one-dimensional structure consisting of edge-shared tetrahedral, while BeF_2 has a three-dimensional structure [31].

The Bader charge analysis of the Be atom shows that the largest charge is found in the $\text{Be}@C_{60}$ structure, while the Be^{++} ion has the lowest charge.

IV. CONCLUSIONS

In this study, the ADF package was used to determine the average electron density at the nucleus. First-principle

calculations based on the DFT method show that the electron density at the ${}^7\text{Be}$ nucleus can be varied by the geometrical position change of ${}^7\text{Be}$ in the fullerene structure. Moreover, it was found that the smallest electron density at the ${}^7\text{Be}$ nucleus is found in ${}^7\text{Be}@C_{36}$; therefore, the half-life of the ${}^7\text{Be}$ nucleus is the largest in this compound. Electron density in ${}^7\text{Be}@C_{60}$ is larger than ${}^7\text{Be}-C_{60}$ due to the existence of many π electrons in C_{60} . Furthermore, the decay rate of the ${}^7\text{Be}$ is considerably decreased by interacting with high electronegativity atoms.

Moreover, the fluorine atom has the most electronegativity among all atoms; therefore, electron density at the Be nucleus is considerably decreased by its interaction. Also, more decrease in electron density is predicted for a higher number of fluorine atoms.

-
- [1] E. Segrè, *Phys. Rev.* **71**, 274 (1947).
 [2] R. Daudel, *Rev. Sci.* **85**, 162 (1947).
 [3] E. Segrè and C. E. Wiegand, *Phys. Rev.* **75**, 39 (1949).
 [4] J. J. Kraushaar, E. D. Wilson, and K. T. Bainbridge, *Phys. Rev.* **90**, 610 (1953).
 [5] C.-A. Huh, *Earth Planet. Sci. Lett.* **171**, 325 (1999).
 [6] A. V. Bibikov, A. V. Avdeenkov, I. V. Bodrenko, A. V. Nikolaev, and E. V. Tkalya, *Phys. Rev. C* **88**, 034608 (2013).
 [7] H. W. Johlige, D. C. Aumann, and H.-J. Born, *Phys. Rev. C* **2**, 1616 (1970).
 [8] J. Tossell, *Earth Planet. Sci. Lett.* **195**, 131 (2002).
 [9] B. Wang, S. Yan, B. Limata, F. Raiola, M. Aliotta, H. Becker, J. Cruz, N. De Cesare, A. D'Onofrio, Z. Fülöp *et al.*, *Eur. Phys. J. A* **28**, 375 (2006).
 [10] A. Ray, P. Das, S. Saha, S. Das, B. Sethi, A. Mookerjee, C. Chaudhuri, and G. Pari, *Phys. Lett. B* **455**, 69 (1999).
 [11] V. Kumar, M. Hass, Y. Nir-El, G. Haquin, and Z. Yungreiss, *Phys. Rev. C* **77**, 051304(R) (2008).
 [12] E. Norman, G. Rech, E. Browne, and R. Larimer, *Phys. Lett. B* **519**, 15 (2001).
 [13] H. W. Kroto, J. R. Heath, S. C. O'Brien, R. F. Curl, and R. E. Smalley, *Nature (London)* **318**, 162 (1985).
 [14] A. Ito, T. Monobe, T. Yoshii, and K. Tanaka, *Chem. Phys. Lett.* **315**, 348 (1999).
 [15] D. L. Huang, P. D. Dau, H. T. Liu, and L. S. Wang, *J. Chem. Phys.* **140**, 224315 (2014).
 [16] T. Ohtsuki, H. Yuki, M. Muto, J. Kasagi, and K. Ohno, *Phys. Rev. Lett.* **93**, 112501 (2004).
 [17] A. Ray, P. Das, S. K. Saha, S. K. Das, J. J. Das, N. Madhavan, S. Nath, P. Sugathan, P. V. M. Rao, and A. Jhingan, *Phys. Rev. C* **73**, 034323 (2006).
 [18] T. Ohtsuki, K. Ohno, T. Morisato, T. Mitsugashira, K. Hirose, H. Yuki, and J. Kasagi, *Phys. Rev. Lett.* **98**, 252501 (2007).
 [19] J. Lu, Y. Zhou, X. Zhang, and X. Zhao, *Chem. Phys. Lett.* **352**, 8 (2002).
 [20] E. V. Tkalya, A. V. Bibikov, and I. V. Bodrenko, *Phys. Rev. C* **81**, 024610 (2010).
 [21] E. V. Tkalya, A. V. Avdeenkov, A. V. Bibikov, I. V. Bodrenko, and A. V. Nikolaev, *Phys. Rev. C* **86**, 014608 (2012).
 [22] A. V. Bibikov, A. V. Nikolaev, and E. V. Tkalya, *Phys. Rev. C* **100**, 064603 (2019).
 [23] M. S. T. Bukowinski, *Geophys. Res. Lett.* **6**, 697 (1979).
 [24] K. Lee and G. Steinle-Neumann, *Earth Planet. Sci. Lett.* **267**, 628 (2008).
 [25] T. Morisato, K. Ohno, T. Ohtsuki, K. Hirose, M. Sluiter, and Y. Kawazoe, *Phys. Rev. B* **78**, 125416 (2008).
 [26] Y. Zhao and D. G. Truhlar, *J. Chem. Phys.* **125**, 194101 (2006).
 [27] G. te Velde, F. M. Bickelhaupt, E. J. Baerends, C. Fonseca Guerra, S. J. A. van Gisbergen, J. G. Snijders, and T. Ziegler, *J. Comput. Chem.* **22**, 931 (2001).
 [28] F. Goldfarb, C. Drag, W. Chaibi, S. Kröger, C. Blondel, and C. Delsart, *J. Chem. Phys.* **122**, 014308 (2005).
 [29] F. Richard and R. Bader, *Atoms in Molecules: A Quantum Theory* (Oxford University Press, Oxford, 1990).
 [30] F. Jensen, *Introduction to Computational Chemistry*, 3rd ed. (John Wiley & Sons, 2017).
 [31] U. Müller, *Inorganic Structural Chemistry*, 2nd ed. (John Wiley & Sons, 2006).